

Dopamine-Based Paper Analytical Device for Truly Equipment-Free and Naked-Eye Biosensing Based on the Target-Initiated Catalyzed Oxidation

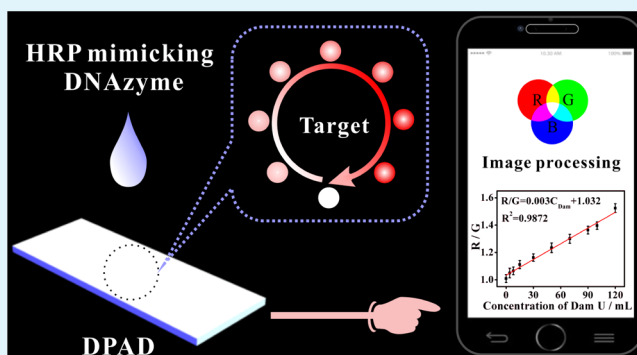
Haiyin Li, Haiyang Lin, Xin Wang, Wenxin Lv, and Feng Li*

College of Chemistry and Pharmaceutical Sciences, Qingdao Agricultural University, Qingdao 266109, People's Republic of China

S Supporting Information

ABSTRACT: The development of low cost, portable, and disposable biosensors for equipment-free and naked-eye biosensing is in eager demand for their widespread application in biomedical field, but it is still a challenge. Herein, we propose a novel paper analytical device (PAD) for truly equipment-free and naked-eye biosensing using dopamine as the chromogenic agent based on target-initiated catalyzed oxidation reaction. The dopamine-functionalized PAD (DPAD) possesses a significant three-dimensional net structure, excellent hydrophilicity, and unique response toward G-quadruplex DNAs against other DNAs, benefiting the bio/chemo reaction occurrence to assay target biomolecules. In light of the exceptional properties, the fabricated DPAD was applied in the analysis of Dam MTase through target-triggered exponential isothermal amplification. The recognition and methylation of H1 by Dam MTase contribute to formation of abundant hemin/G-quadruplexes, which catalyze oxidation of dopamine into dopachrome and reduce the dopamine amount on the DPAD surface. In comparison with the case in which Dam MTase is absent, an evident deep pink signal originating from dopachrome is observed directly by the naked eye and relied on Dam MTase concentrations. Therefore, truly equipment-free and naked-eye detection of Dam MTase is achieved with a detection limit of 1.46 U/mL. The fabricated DPAD not only achieves Dam MTase-visualized detection but also permits the accurate determination of other analytes by varying recognizable DNA's sequences, thus offering a universal biosensor and depicting significant potential for widespread applications in biomedical field.

KEYWORDS: paper analytical device, equipment-free, naked-eye, Dam MTase, dopamine



INTRODUCTION

With increasing concerns on human health and public safety, there is great demand for simple, accurate, and sensitive detection of disease-related biomarkers.^{1–3} Aiming at this problem, a large number of biosensors (fluorescence, ultraviolet, photoelectrochemistry, electrochemistry, surface plasmon resonance, and so on) were reported and devoted to assaying these biomarkers.^{4–9} For instance, Zhu et al. realized the tumor-related ncRNA sensitive detection based on a universal upconversion sensing platform.¹⁰ Tang et al. reported a visible carcinoembryonic antigen assay using the fluorescence immunoassay method.¹¹ Although these biomarkers have been sensitively and selectively detected, there are still some insurmountable problems associated with the present biosensors.^{12–15} (1) These sensing strategies are limited to large-scale instruments, which are high-end, complex, and expensive. (2) They need professional technicians to operate the equipments and analyze the experimental information, counting against universal applications. (3) Their diagnostic processes mainly focus on solution-phase systems, which are unstable and adverse for practical applications outside the

laboratory. Undoubtedly, these obstacles infinitely prevent the large-scale applications of abovementioned biosensors outside the laboratory and are bad for on-site/real-time/rapid diagnosis of various diseases. In response to the issues mentioned above, we endeavor, here, to devise a simple, equipment-free, and naked-eye solid biosensor based on cellulose paper for a highly sensitive detection of disease-related biomarkers.

Cellulose paper has experienced rapid development in the past few years because of its intrinsic promising specialties: low cost, portability, disposability, and user-friendliness. Moreover, it has a porous structure, which is favorable for it to act as matrix to conduct bio/chemo reactions. From this context, combining cellulose paper with various sensing strategies not only reduces the cost of testing but also realizes the visualized detection of target biomarkers.^{16–19} Thus, substantial efforts have been devoted to the cellulose paper analytical device

Received: August 19, 2019

Accepted: September 23, 2019

Published: September 23, 2019



(PAD), and tremendous progress has been achieved in the field of disease diagnosis. The previously reported PADs primarily concentrated on colorimetric, fluorescent, electrochemical, and surface-enhanced Raman scattering techniques.^{20–24} Among them, colorimetric PADs are regarded as ideal tools because of the truly equipment-free and naked-eye characteristics, which not only lower the cost of testing and simplify the process of testing but also boost the large-scale and universal application outside the laboratory. For example, Mahato and Chandra reported a naked-eye alkaline phosphatase detection method using a paper-based miniaturized immunosensor.²⁵ Despite the simple and effective analysis, these colorimetric PADs suffered from the relatively low sensitivity, which impedes their broader applications because of the low expression level of biomarkers in biological liquids. In view of this, there is great demand for developing colorimetric PADs with high sensitivity. It is well known that sensing performance of colorimetric PADs mostly depends upon the properties of selected chromogenic agents. Dopamine is an organic molecule with $-\text{NH}_2$ and $-\text{OH}$ in the benzene ring and is mainly applied as the raw material to prepare polydopamine through catalyzing oxidation reaction. Existing studies suggested that polydopamine has been widely utilized in the fields of energy storage, catalysis, environmental pollution, bio/chemo-analysis, and disease treatment.²⁶ Recently, it was reported that dopamine can be catalytically oxidized into dopachrome in mildly acidic solution with the aid of H_2O_2 and horseradish peroxidase (HRP), accompanied with the change in color of the discolored solution from colorless to deep pink.^{27,28} Consequently, by making the best of the outstanding discoloration characteristic, dopamine can be used as an ideal chromogenic agent to develop colorimetric PADs with high sensitivity.

Another effective method to improve detection sensitivity is the enzyme-assisted signal amplification strategy, such as exponential amplification reaction (EXPAR), exonuclease III digestion reaction, polymerase chain reaction, and rolling circle amplification reaction.^{29–33} Among them, EXPAR plays a key role in signal amplification because of its intrinsic merits. (1) EXPAR combines the advantages of polymerase-assisted strand extension and nicking enzyme-mediated strand release, which make for the high sensitivity; (2) EXPAR could realize the 10^6 to 10^9 -fold signal amplification only for several minutes, benefitting the on-site/real-time/rapid analysis; (3) EXPAR can be successfully carried out under isothermal conditions. Taking into account these outstanding features, we have reasons to believe that the EXPAR strategy can be used as an ideal signal amplification tool to improve colorimetric PADs' sensitivity.

Enlightened by the aforementioned investigations, herein, we proposed a novel PAD (DPAD) for truly equipment-free and naked-eye biosensing using dopamine (Figure S1A) as the chromogenic agent. The DPAD was fabricated through a single-step drop-coating method and exhibited unique response toward hemin/G-quadruplex (HRP mimicking enzyme) in the presence of H_2O_2 via target-triggered catalyzed oxidation reaction. For the abovementioned reason, the DPAD was employed as a biosensor for Dam MTase (related with cell proliferation and gene expression) assaying, used as the model target, which triggers the EXPAR to produce large numbers of hemin/G-quadruplexes with the help of K^+ .^{34–37} This study allows the readout signal to be observed directly by the naked

eye and thus holds a great potential for large-scale and universal applications in an undeveloped area.

EXPERIMENTAL SECTION

Fabrication of DPAD. Dopamine solution was prepared through dissolving dopamine hydrochloride in 10 mM phosphate buffer (pH 7.0) to generate a concentration of 20 mM. Subsequently, the DPAD was fabricated via dropping 3 μL of dopamine solution on the surface of cellulose paper. The DPAD was then dried in a vacuum environment at 4 $^\circ\text{C}$ for 12 h.

Detection of G-Quadruplex DNA Using the DPAD. The G-quadruplex DNA assay was carried out in 85 μL of 10 mM Tris-HCl reaction solution (50 mM NaCl, 50 mM MgCl_2 , 100 mM KCl, pH 7.4) containing 4.70 μM hemin and target G-quadruplex DNA with different concentrations to generate hemin/G-quadruplexes. After that, 15 μL of H_2O_2 (60 mM) solution was added into the above solution. After complete mixing, 3 μL of the resulting solution was dropped on the surface of the DPAD and reacted for 20 s. Then, the images of the DPAD were obtained using a mobile phone (Huawei Mate 20), and the signal intensity was read directly by the naked eye for equipment-free detection of G-quadruplex DNA.

Detection of Dam MTase Activity Using the DPAD. The Dam MTase-initiated methylation reaction was performed in 20 μL of 10 mM Tris-HCl reaction solution (50 mM NaCl, 10 mM MgCl_2 , pH 7.5) containing 10 μM HI, 1.0 mM dithiothreitol (DTT), 0.8 mM S-adenosylmethionine (SAM), 500 U/mL Dpn I, and target Dam MTase with different concentrations for 2.0 h. After that, 50 μL of 10 mM Tris-HCl solution (50 mM NaCl, 50 mM MgCl_2 , 100 mM KCl, 1 mM DTT, pH 7.5) comprising 8.0 μM P1, 1.0 U/ μL KF polymerase, 6.0 U/ μL Nb.BbvCI NEase, and 3.5 mM deoxynucleotide (dNTP) was added and reacted for 1.5 h to complete the EXPAR. The mixture was then heated to 90 $^\circ\text{C}$ and maintained at 90 $^\circ\text{C}$ for 10 min to eliminate the influence of DTT. Then, 15 μL of 26.60 μM hemin was incubated with it for 45 min to generate hemin/G-quadruplexes. Another 15 μL of H_2O_2 solution (60 mM) was fully mixed with hemin/G-quadruplex solution to prepare the resulting solution. Finally, 3 μL of the resulting solution was dropped on the surface of the DPAD and reacted for 20 s. Then, the images of DPAD were obtained using the mobile phone (Huawei Mate 20), and the RGB (red, green, and blue) values were recorded from a Color Picker APP in the mobile phone.

RESULTS AND DISCUSSION

Characterizations of DPAD. DPAD was fabricated following the schematic illustration manifested in Figure 1A,

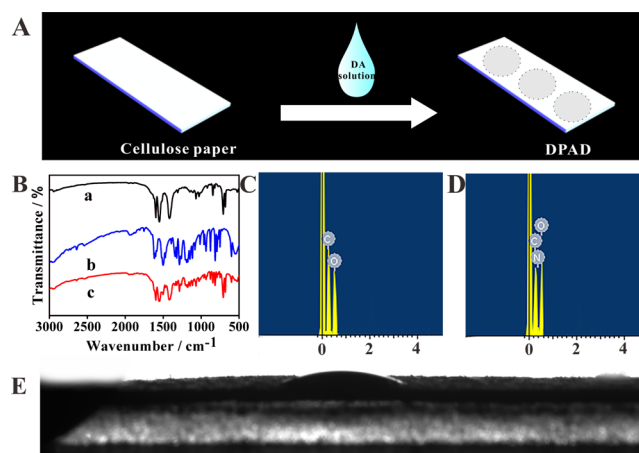


Figure 1. (A) Schematic illustration for DPAD fabrication. (B) FT-IR spectra of (a) cellulose paper, (b) dopamine, and (c) DPAD. (C) EDS of cellulose paper. (D) EDS of the DPAD. (E) Contact angle of the DPAD.

and the detailed processes for its preparation are shown in the [Experimental Section \(Fabrication of DPAD\)](#). In this strategy, dopamine, which could specifically recognize G-quadruplex DNA, was immobilized on cellulose paper's surface via the drop-coating method. The immobilization of dopamine on paper's surface was verified by Fourier transform infrared (FT-IR) spectra. As depicted in [Figure 1B](#), new peaks 708, 1278, and 1493 cm^{-1} , belonging to characteristic peaks of dopamine, appeared in the spectrum of the DPAD compared with that of cellulose paper, justifying the triumphant modification of dopamine on cellulose paper's surface. To further confirm the attachment of dopamine to paper, the energy dispersive spectroscopy (EDS) technique was conducted. Evidently, there are two peaks existing in the EDS spectrum of cellulose paper, which correspond well to C and O elements and are consistent with paper's molecular structure. After the modification of dopamine, new peak 0.3920 keV belonging to N element appeared. This newly appearing peak directly proved that dopamine was immobilized on the surface of cellulose paper.

To gain more insights into DPAD, scanning electron microscopy (SEM) and contact angle measurements were conducted to evaluate the morphology and hydrophilicity/hydrophobicity. As shown in [Figure S2](#), a three-dimensional network of cellulose fibers with a diameter of 5 μm was observed for cellulose paper and DPAD. Meanwhile, the DPAD enjoyed excellent hydrophilicity with the contact angle of 8.7°, which is comparable to that of cellulose paper alone. These experimental results suggested that dopamine had little influence on the morphology and hydrophilicity of the used paper, thus aiding the DPAD to conduct the bio/chemo reactions and improve detection sensitivity.

Study of the G-Quadruplex DNA-Responsive Property of the DPAD. On the ground of the fabricated DPAD, analysis of G-quadruplex DNA via target-initiated catalyzing oxidation reaction was proposed ([Figure 2A](#)). In the presence

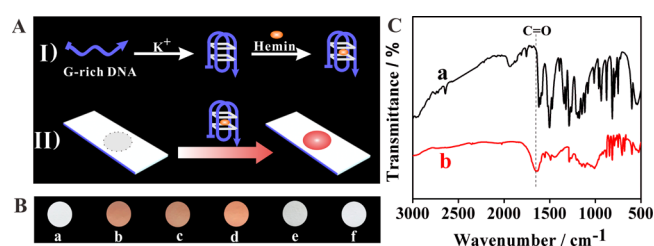


Figure 2. (A) Principle of DPAD for G-quadruplex DNA biosensing. (B) Images of DPAD under different conditions: (a) blank sample, (b) T1, (c) T2, (d) T3, (e) T4, (f) T5. The concentrations of them are 400 nM. (C) FT-IR spectra of dopamine under different conditions: (a) in the absence of T1 and (b) in the presence of T1.

of the target analyte, large amounts of hemin/G-quadruplexes will be formed with the aid of K⁺. Hemin/G-quadruplex possesses significant HRP-like activity, and thus can catalyze oxidation of dopamine into dopachrome ([Figure S1B](#)) with H₂O₂ as the coreactant, contributing to a significant color change from white to deep pink. Nevertheless, when G-quadruplex DNA was not added into the sensing system, the DPAD maintained its color unchanged because of no generation of hemin/G-quadruplex. Evidently, deep pink was related to the catalytic oxidation product dopachrome, which subsequently depended on target G-quadruplex DNA. Thus,

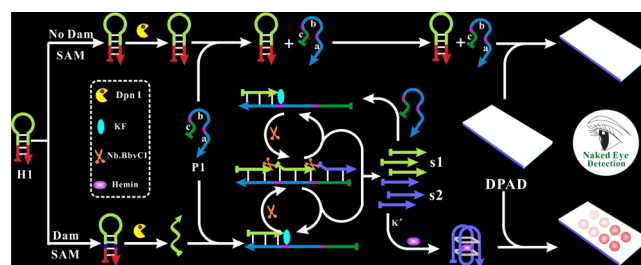
naked-eye analysis of G-quadruplex DNA can be readily realized through the color change based on the DPAD.

To confirm the feasibility of the DPAD for G-quadruplex DNA analysis, some experiments were carried out using T1 as the model analyte, which can be intercalated with hemin tightly to produce the HRP-mimicking DNAzyme. As depicted in [Figure 2B](#), the significant deep pink signal (image b) was determined when T1 was added into the sensing system with the assistance of K⁺, hemin, and H₂O₂, compared with that of the blank sample (image a). It is no wonder that the sensing mechanism was derived from hemin/G-quadruplexes' ability to efficiently catalyze oxidation of dopamine into dopachrome, as well as the color difference of dopamine and dopachrome. The catalyzed oxidation of dopamine by hemin/G-quadruplex can also be verified by ultraviolet–visible (UV–vis) ([Figure S3A](#)) and FT-IR characterizations ([Figure 2C](#)). Obviously, a new absorption peak located at 475 nm, corresponding to dopachrome, appeared when T1 was present in the sensing system. In addition, much stronger absorbance than that of the blank sample was obtained. Furthermore, a new FT-IR peak located at 1609 cm^{-1} , corresponding to carbonyl in dopachrome, appeared in the spectrum of the DPAD after the treatment of T1.

According to the working principle, it is inferred that the fabricated DPAD can be employed as an effective biosensor for differentiating G-quadruplex DNAs against other DNAs through identifying the changed color. With the aim to obtain more information, we conducted the experimental investigation of the DPAD subjected to different target DNAs with their sequences shown in [Table S1](#), namely, T2, T3, T4, and T5 ([Figure 2B](#)). As expected, DPAD's color changed to deep pink only in the presence of T2 and T3. When T4 or T5 existed in the sensing system, the color of the DPAD changed negligibly compared with that of the blank sample because of no generation of hemin/G-quadruplex. Similar conclusion can be also obtained from UV–vis measurements in solution ([Figure S3B](#)). Overall, the fabricated DPAD possesses specific color recognition ability toward G-quadruplex DNAs.

Naked-Eye Detection of Dam MTase Based on the DPAD. Owing to specific response of the DPAD toward G-quadruplex DNA, it is expected that the fabricated DPAD can be applied in the sensitive detection of various analytes, which can trigger enzyme-mediated signal transduction and amplification reactions to generate abundant G-quadruplex DNAs. In the present study, Dam MTase was used as the proof-of-concept analyte, and the scheme for Dam MTase naked-eye detection based on DPAD was depicted in [Scheme 1](#). Both H1 and P1 were carefully designed so that they could eliminate the

Scheme 1. Schematic Illustration of the Principle of the DPAD for Dam MTase Detection Based on Target-Switched EXPAR Reaction



spontaneous reaction between each other in the absence of target Dam MTase. In addition, H1 contains the sequences of 5'-GATC-3' in dsDNA recognized by Dam MTase; P1 contains three domains (a, b, and c) divided by two Nb.BbvCI recognition sites, of which a and b domains possess the same sequences complementary to the chartreuse fragment embedded in H1, and c domain comprises the sequences hybridizing with G-quadruplex DNA. In the absence of target Dam MTase, H1 and P1 maintained their configurations unchanged, which can be verified by the gel electrophoresis characterization (Figure 3A lane a, b, and c). Because no G-

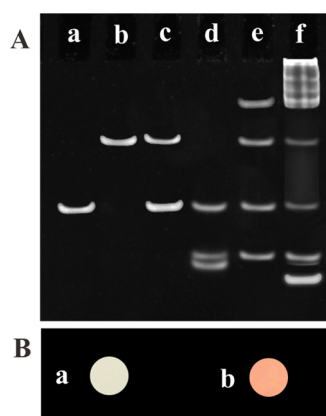


Figure 3. (A) Nondenaturing polyacrylamide gel electrophoresis images of (a) H1, (b) P1, (c) H1 + P1, (d) H1 + SAM + Dam MTase + Dpn I, (e) H1 + SAM + Dam MTase + Dpn I + P1, and (f) H1 + SAM + Dam MTase + Dpn I + P1 + KF polymerase + dNTPs + Nt.BbvCI. (B) Images of the DPAD under different conditions: (a) in the absence of Dam MTase and (b) in the presence of Dam MTase.

quadruplex DNA was produced, the color of the DPAD did not change. However, upon the addition of target Dam MTase into the system, H1 was efficiently cleaved into both red and chartreuse fragments, confirmed by the newly appearing bands in the front of H1 (lane d). The chartreuse fragment in turn hybridized with the a or b region in P1 to generate the complex, thus contributing to the appearance of the band behind that of P1 (lane e). Under such circumstances, the target-initiated cleavage product, the chartreuse fragment, served as the primer to initiate the EXPAR reactions, generating abundant DNA triggers. Because of the exquisite plan, s1 hybridized with unused P1 to trigger more EXPAR to produce more s2. It stands to reason that many new bands appeared at different locations (lane f), and among them, the foremost band was deemed as the G-quadruplex DNAs s2. As a consequence, large numbers of hemin/G-quadruplexes generated via the K^+ -guided conformation change and hemin's excellent intercalation ability in G-quadruplex, and subsequently catalyzed oxidation of dopamine into dopachrome, contributing to the increased deep pink signal. From this context, by determining the color change, we could achieve the truly equipment-free and naked-eye detection of Dam MTase with high sensitivity by combining the fabricated DPAD with EXPAR.

To confirm the feasibility of the fabricated DPAD for Dam MTase biosensing, different experiments were carried out in the absence/presence of target Dam MTase with the concentration of 120 U/mL (Figure 3B). After reaction with mixed solution containing H1, P1, H_2O_2 , hemin, KF

polymerase, Nb.BbvCI, and dNTPs, the DPAD showed a slight color change compared with the DPAD alone. Nevertheless, when Dam MTase was added into the mixed solution, a significant deep pink signal was observed, strongly justifying the feasibility for naked-eye detection of Dam MTase using the DPAD. The proposed strategy can be also verified by UV-vis spectra in solution (Figure S4). Furthermore, when A1 or B1 or C1 replaced H1 to detect Dam MTase, the DPAD displayed a white signal and the sensing system showed low absorbance in solution (Figure S5), confirming the importance of the H1 structure for Dam assay development. Subsequently, a series of solutions containing different Dam MTase concentrations were added into the reaction system to evaluate the DPAD's sensing performance, and the experimental results are shown in Figure 4. Evidently, the deep pink level enhanced

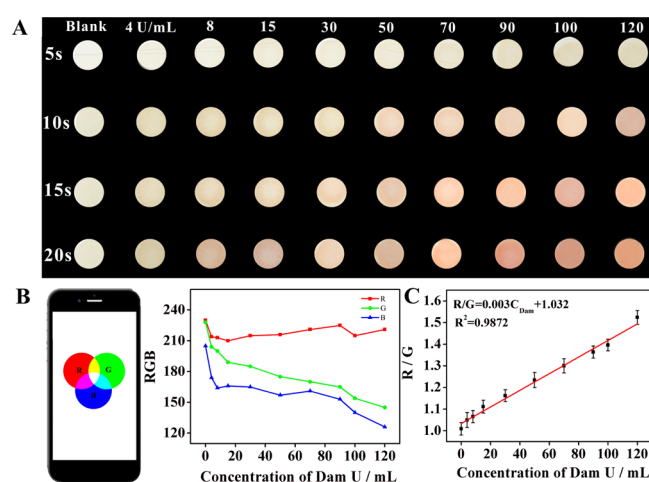


Figure 4. (A) Images of the DPAD corresponding to different amounts of Dam MTase under different reaction time points. (B) RGB values of DPAD corresponding to different amounts of Dam MTase. (C) Working curve of the R/G ratio and Dam MTase concentrations.

with the increase of Dam MTase concentration, corresponding well to the working mechanism that more Dam MTase guided more HRP-mimicking DNazymes' generation and subsequently consumed more dopamine into dopachrome, thus strengthening the deep pink signal. In addition, it is worth noting that 20 s is sufficient for completing the color reaction on the DPAD surface, benefiting the rapid/on-site detection. From the minimum deep pink signal read directly by the naked eye, Dam MTase concentration was 4.0 U/mL. To realize quantitative analysis, RGB values of the DPAD corresponding to different Dam MTase amounts were obtained from the Color Picker APP. Figure 4B displayed the values of blue "B" and green "G" decreased with Dam MTase concentration increasing, accompanied with that the intensity of red "R" keep practically unchanged. By using the R/G ratio as the vertical coordinate and the Dam MTase amount (C_{Dam}) as the horizontal coordinate (Figure 4C), the working curve was drafted in the range of 4–120 U/mL with equation of $R/G = 0.003C_{Dam} + 1.032$ and the coefficient of 0.9872. Also, the detection limit (LOD) was calculated to be 1.46 U/mL based on the signal to noise of three. Although the LOD was higher than that of the corresponding UV-vis method (0.023 U/mL, Figure S6) and other techniques reported previously (Table S2), the fabricated DPAD enjoyed inexpensive, equipment-

free, and visualized characteristics, and moreover, met the demand for Dam MTase assaying in biological liquids.³⁸

Further, M.Sss I, M. CviP I, and MsP I MTases were chosen as interfering substances to evaluate the selectivity of the DPAD for Dam MTase (Figure 5A). These proteins belong to

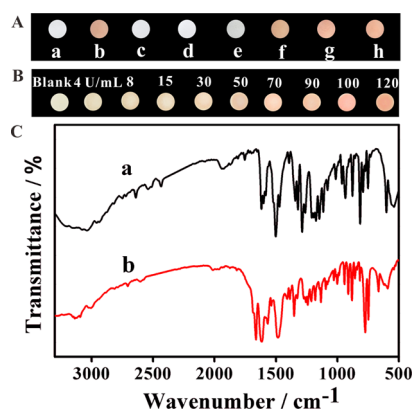


Figure 5. (A) Selectivity experiment of the established DPAD subject to different MTases. The concentrations of all MTases were 120 U/mL. (a) Blank sample, (b) Dam, (c) M.Sss I, (d) M. CviP I, (e) MsP I, (f) Dam + M.Sss I, (g) Dam + M. CviP I, and (h) Dam + MsP I. (B) Stability experiment of the DPAD after the storage at 4 °C for 7.0 days subject to different concentrations of Dam MTase. (C) FT-IR curves of (a) dopamine and (b) DPAD after the storage at 4 °C for 7.0 days.

the MTase family and possess excellent methylation ability on specific DNA sequences. For the elaborate design of the H1 sequence, color signals for M.Sss I, M. CviP I, and MsP I were the same with that of the blank sample, suggesting that the three interferences could not recognize the sequence of 5'-GATC-3' in H1. However, upon the addition of Dam MTase, an obvious deep pink signal was detected because of the high specificity of methylation sequences. More importantly, when interfering proteins were mixed with Dam MTase, they had negligible influence on the sensing performance of the DPAD toward Dam MTase. Further, similar phenomena can be also observed from UV-vis information in the solution state (Figure S7). These results firmly suggested that the fabricated DPAD enjoys good specificity toward Dam MTase and can differentiate Dam MTase against other MTases through the ingenious design of DNA sequences. Stability is another indispensable assessment criterion for developed biosensors. Thus, we test the stability of the DPAD by storing it at 4 °C for 7.0 and 14.0 days (Figures 5B and S8). It was found that there was no color change on the DPAD surface in the absence of Dam, implying no reaction occurrence and good stability. The stability can be also verified by FT-IR curves, in which no new peaks corresponding to carbonyl appeared (Figure 5C). To gain more insights into the stability of the DPAD, we challenged the stored DPAD via detecting Dam MTase with different amounts. The deep pink signal was similar to that obtained from the ready-to-use DPAD under the same conditions.

In view of the fascinating properties, the DPAD was applied in analysis of Dam MTase in biological fluid through the spiking method, and the biological sample was prepared through the equal volume mixing of human serum and Tris-HCl. As depicted in Figure S9A, weak or no deep pink signal appeared in the absence of target Dam MTase, implying the

good anti-interference ability of the DPAD toward serum. Further, when Dam MTase with the amount of 40 and 120 U/mL was added into the reaction solution, the deep pink signal appeared and heightened with the increased Dam MTase activity. This information verified the fabricated DPAD as an ideal candidate for Dam MTase biosensing in biological fluid. The fabricated DPAD could be also applied for MTase inhibitor screening, using 5-fluorouracil, benzylpenicillin, and gentamycin as the model inhibitors. After pre-incubation with Dam MTase, significantly decreased deep pink signals were observed for 5-fluorouracil, benzylpenicillin, and gentamycin, justifying the effective inhibition on Dam MTase activity (Figure S9B). Meanwhile, in Figure S9C, it can be seen that the deep pink signal of the DPAD reduced with the increase of 5-fluorouracil concentration, corresponding well to the fact that more 5-fluorouracil would prohibit more Dam MTase, thus hampering dopachrome's generation. Thus, using the fabricated DPAD, equipment-free and naked-eye screening of MTase inhibitors can be readily achieved.

CONCLUSIONS

In summary, a novel solid biosensor has been designed and fabricated for truly equipment-free and naked-eye biosensing based on target-initiated catalyzing oxidation reaction and in situ-generated product-mediated signal readout/enhancement strategy. With cellulose paper and dopamine taken as the reaction matrix and chromogenic agent, respectively, the DPAD was successfully fabricated through the drop-coating method with the features such as low cost, disposability, equipment-free, and visual inspection by the naked eye, and presented unique responsive ability toward G-quadruplex DNAs against other DNAs. Because of the excellent properties of the DPAD, we demonstrated its application in the naked-eye analysis of Dam MTase, used as the model target analyte, based on the target-initiated EXPAR. The experimental results implied that the deep pink signal was positively proportional to Dam MTase concentrations, and the LOD was calculated to be 1.46 U/mL, meeting the demand for Dam MTase assaying in biological fluid. Moreover, the fabricated DPAD possessed good stability and exceptional specificity on Dam MTase against other MTases and was successfully applied in screening MTase inhibitors and analysis of Dam MTase in human serum. Therefore, the fabricated DPAD enjoys significant potential for large-scale and universal applications in the field of biomedical engineering.

ASSOCIATED CONTENT

Supporting Information

The Supporting Information is available free of charge on the ACS Publications website at DOI: 10.1021/acsami.9b14859.

DNA sequences; Dam MTase assay performance; SEM characterization; UV-vis characterization (PDF)

AUTHOR INFORMATION

Corresponding Author

*E-mail: lifeng@qau.edu.cn. Phone/Fax: 86-532-86080855.

ORCID

Feng Li: 0000-0002-3894-6139

Notes

The authors declare no competing financial interest.

■ ACKNOWLEDGMENTS

This work was funded by the National Natural Science Foundation of China (21605093 and 21775082), the Special Foundation for Distinguished Taishan Scholar of Shandong Province (ts201511052), and the Major Program of Shandong Province Natural Science Foundation (ZR2018ZC0127).

■ REFERENCES

- (1) Das, P. M.; Singal, R. DNA Methylation and Cancer. *J. Clin. Oncol.* **2004**, *22*, 4632–4642.
- (2) Wu, L.; Qu, X. Cancer Biomarker Detection: Recent Achievements and Challenges. *Chem. Soc. Rev.* **2015**, *44*, 2963–2997.
- (3) Chinen, A. B.; Guan, C. M.; Ferrer, J. R.; Barnaby, S. N.; Merkel, T. J.; Mirkin, C. A. Nanoparticle Probes for the Detection of Cancer Biomarkers, Cells, and Tissues by Fluorescence. *Chem. Rev.* **2015**, *115*, 10530–10574.
- (4) Feng, Q.; Zhao, X.; Guo, Y.; Liu, M.; Wang, P. Stochastic DNA Walker for Electrochemical Biosensing Sensitized with Gold Nanocages@Graphene Nanoribbons. *Biosens. Bioelectron.* **2018**, *108*, 97–102.
- (5) Xu, Z.-Q.; Zhang, P.; Chai, Y.-Q.; Wang, H.-J.; Yuan, R. A Biosensor Based on a 3D-DNA Walking Machine Network and Distance-Controlled Electrochemiluminescence Energy Transfer for Ultrasensitive Detection of Tenascin C and Lead Ions. *Chem. Commun.* **2018**, *54*, 8741–8744.
- (6) Chang, J.; Wang, X.; Wang, J.; Li, H.; Li, F. Nucleic Acid-Functionalized Metal–Organic Framework-Based Homogeneous Electrochemical Biosensor for Simultaneous Detection of Multiple Tumor Biomarkers. *Anal. Chem.* **2019**, *91*, 3604–3610.
- (7) Wang, X.; Li, P.; Ding, Q.; Wu, C.; Zhang, W.; Tang, B. Illuminating the Function of the Hydroxyl Radical in the Brains of Mice with Depression Phenotypes by Two-Photon Fluorescence Imaging. *Angew. Chem.* **2019**, *58*, 4674–4678.
- (8) Li, H.; Wang, C.; Hou, T.; Li, F. Amphiphile-Mediated Ultrasmall Aggregation Induced Emission Dots for Ultrasensitive Fluorescence Biosensing. *Anal. Chem.* **2017**, *89*, 9100–9107.
- (9) Rull-Barrull, J.; d'Halluin, M.; Le Grogne, E.; Felpin, F.-X. Chemically-Modified Cellulose Paper as Smart Sensor Device for Colorimetric and Optical Detection of Hydrogen Sulfate in Water. *Chem. Commun.* **2016**, *52*, 2525–2528.
- (10) Zhang, K.; Yang, L.; Lu, F.; Wu, X.; Zhu, J.-J. A Universal Upconversion Sensing Platform for the Sensitive Detection of Tumour-Related Ncrna through an Exo III-Assisted Cycling Amplification Strategy. *Small* **2018**, *14*, 1703858.
- (11) Lv, S.; Tang, Y.; Zhang, K.; Tang, D. Wet NH₃-Triggered NH₂-MIL-125(Ti) Structural Switch for Visible Fluorescence Immunoassay Impregnated on Paper. *Anal. Chem.* **2018**, *90*, 14121–14125.
- (12) Kwon, H.; Samain, F.; Kool, E. T. Fluorescent DNAs Printed on Paper: Sensing Food Spoilage and Ripening in the Vapor Phase. *Chem. Sci.* **2012**, *3*, 2542–2549.
- (13) Song, Y.; Gyarmati, P.; Araújo, A. C.; Lundberg, J.; Brumer, H., III; Ståhl, P. L. Visual Detection of DNA on Paper Chips. *Anal. Chem.* **2014**, *86*, 1575–1582.
- (14) Rojas, J. P.; Conchouso, D.; Arevalo, A.; Singh, D.; Foulds, I. G.; Hussain, M. M. Paper-Based Origami Flexible and Foldable Thermoelectric Nanogenerator. *Nano Energy* **2017**, *31*, 296–301.
- (15) Jia, R.; Tian, W.; Bai, H.; Zhang, J.; Wang, S.; Zhang, J. Amine-Responsive Cellulose-Based Ratiometric Fluorescent Materials for Real-Time and Visual Detection of Shrimp and Crab Freshness. *Nat. Commun.* **2019**, *10*, 795.
- (16) Parolo, C.; Merkoçi, A. Paper-Based Nanobiosensors for Diagnostics. *Chem. Soc. Rev.* **2013**, *42*, 450–457.
- (17) Reddy G, U.; Liu, J.; Hoffmann, P.; Steinmetz, J.; Görls, H.; Kupfer, S.; Askes, S. H. C.; Neugebauer, U.; Gräfe, S.; Schiller, A. Light-Responsive Paper Strips as CO-Releasing Material with a Colourimetric Response. *Chem. Sci.* **2017**, *8*, 6555–6560.
- (18) Dichiar, A. B.; Song, A.; Goodman, S. M.; He, D.; Bai, J. Smart Papers Comprising Carbon Nanotubes and Cellulose Microfibers for Multifunctional Sensing Applications. *J. Mater. Chem. A* **2017**, *5*, 20161–20169.
- (19) Tawfik, S. M.; Sharipov, M.; Kakhkhorov, S.; Elmasry, M. R.; Lee, Y.-I. Multiple Emitting Amphiphilic Conjugated Polythiophenes-Coated CdTe QDs for Picogram Detection of Trinitrophenol Explosive and Application Using Chitosan Film and Paper-Based Sensor Coupled with Smartphone. *Adv. Sci.* **2019**, *6*, 1801467.
- (20) Amor-Gutiérrez, O.; Costa-Rama, E.; Fernández-Abedul, M. T. Sampling and Multiplexing in Lab-on-Paper Bioelectroanalytical Devices for Glucose Determination. *Biosens. Bioelectron.* **2019**, *135*, 64–70.
- (21) Wang, J.; Dai, J.; Xu, Y.; Dai, X.; Zhang, Y.; Shi, W.; Sellergren, B.; Pan, G. Molecularly Imprinted Fluorescent Test Strip for Direct, Rapid, and Visual Dopamine Detection in Tiny Amount of Biofluid. *Small* **2019**, *15*, 1803913.
- (22) Zeng, Z.-C.; Huang, S.-C.; Wu, D.-Y.; Meng, L.-Y.; Li, M.-H.; Huang, T.-X.; Zhong, J.-H.; Wang, X.; Yang, Z.-L.; Ren, B. Electrochemical Tip-Enhanced Raman Spectroscopy. *J. Am. Chem. Soc.* **2015**, *137*, 11928–11931.
- (23) Yamashige, R.; Kimoto, M.; Okumura, R.; Hirao, I. Visual Detection of Amplified DNA by Polymerase Chain Reaction Using a Genetic Alphabet Expansion System. *J. Am. Chem. Soc.* **2018**, *140*, 14038–14041.
- (24) Wang, F.; Li, W.; Wang, J.; Ren, J.; Qu, X. Detection of Telomerase on Upconversion Nanoparticle Modified Cellulose Paper. *Chem. Commun.* **2015**, *51*, 11630–11633.
- (25) Mahato, K.; Chandra, P. Paper-Based Miniaturized Immunosensor for Naked Eye ALP Detection Based on Digital Image Colorimetry Integrated with Smartphone. *Biosens. Bioelectron.* **2019**, *128*, 9–16.
- (26) Du, X.; Li, L.; Li, J.; Yang, C.; Frenkel, N.; Welle, A.; Heissler, S.; Nefedov, A.; Grunze, M.; Levkin, P. A. UV-Triggered Dopamine Polymerization: Control of Polymerization, Surface Coating, and Photopatterning. *Adv. Mater.* **2014**, *26*, 8029–8033.
- (27) Wang, S.; Cazelles, R.; Liao, W.-C.; Vázquez-González, M.; Zoabi, A.; Abu-Reziq, R.; Willner, I. Mimicking Horseradish Peroxidase and NADH Peroxidase by Heterogeneous Cu²⁺-Modified Graphene Oxide Nanoparticles. *Nano Lett.* **2017**, *17*, 2043–2048.
- (28) Lin, H.; Wang, X.; Wu, J.; Li, H.; Li, F. Equipment-Free and Visualized Biosensor for Transcription Factor Rapid Assay Based on Dopamine-Functionalized Cellulose Paper. *J. Mater. Chem. B* **2019**, *7*, 5461–5464.
- (29) Zhao, Y.; Chen, F.; Li, Q.; Wang, L.; Fan, C. Isothermal Amplification of Nucleic Acids. *Chem. Rev.* **2015**, *115*, 12491–12545.
- (30) Liu, M.; Hui, C. Y.; Zhang, Q.; Gu, J.; Kannan, B.; Jahanshahi-Anbui, S.; Filipe, C. D. M.; Brennan, J. D.; Li, Y. Target-Induced and Equipment-Free DNA Amplification with a Simple Paper Device. *Angew. Chem., Int. Ed.* **2016**, *55*, 2709–2713.
- (31) Cheglakov, Z.; Weizmann, Y.; Basnar, B.; Willner, I. Diagnosing Viruses by the Rolling Circle Amplified Synthesis of Dnazymes. *Org. Biomol. Chem.* **2007**, *5*, 223–225.
- (32) Weizmann, Y.; Cheglakov, Z.; Pavlov, V.; Willner, I. Autonomous Fueled Mechanical Replication of Nucleic Acid Templates for the Amplified Optical Detection of DNA. *Angew. Chem., Int. Ed.* **2006**, *45*, 2238–2242.
- (33) Li, H.; Chang, J.; Gai, P.; Li, F. Label-Free and Ultrasensitive Biomolecule Detection Based on Aggregation Induced Emission Fluorogen Via Target-Triggered Hemin/G-Quadruplex-Catalyzed Oxidation Reaction. *ACS Appl. Mater. Interfaces* **2018**, *10*, 4561–4568.
- (34) Golub, E.; Freeman, R.; Willner, I. A Hemin/G-Quadruplex Acts as a NADH Oxidase and NADH Peroxidase Mimicking Dnazyme. *Angew. Chem., Int. Ed.* **2011**, *50*, 11710–11714.
- (35) Marušič, M.; Plavec, J. The Effect of DNA Sequence Directionality on G-Quadruplex Folding. *Angew. Chem., Int. Ed.* **2015**, *54*, 11716–11719.
- (36) Shimron, S.; Wang, F.; Orbach, R.; Willner, I. Amplified Detection of DNA through the Enzyme-Free Autonomous Assembly

of Hemin/G-Quadruplex Dnzyme Nanowires. *Anal. Chem.* **2012**, *84*, 1042–1048.

(37) Golub, E.; Albada, H. B.; Liao, W.-C.; Biniuri, Y.; Willner, I. Nucleoapzymes: Hemin/G-Quadruplex Dnzyme-Aptamer Binding Site Conjugates with Superior Enzyme-Like Catalytic Functions. *J. Am. Chem. Soc.* **2016**, *138*, 164–172.

(38) Zhang, Y.; Wang, X.-y.; Zhang, Q.; Zhang, C.-y. Label-Free Sensitive Detection of DNA Methyltransferase by Target-Induced Hyperbranched Amplification with Zero Background Signal. *Anal. Chem.* **2017**, *89*, 12408–12415.